REPORT
doi:10.26443/seismica.v2i1.245

Self-sufficient seismic boxes for monitoring glacier seismology

Ana Nap * [1], **Fabian Walter** [2], **Martin P. Lüthi** [1], **Adrien Wehrlé** [1]

[1]Department of Geography, University of Zürich, Zürich, Switzerland, [2]Swiss Federal Institute for Forest, Snow and Landscape Research WSL, Birmersdorf, Switzerland

Author contributions: *Conceptualization*: Ana Nap, Fabian Walter, Martin P. Lüthi. *Formal Analysis*: Ana Nap, Fabian Walter, Adrien Wehrlé. *Writing - Original draft*: Ana Nap. *Visualization*: Ana Nap. *Project administration*: Martin P. Lüthi. *Funding acquisition*: Martin P. Lüthi.

Abstract Glacier seismology is a valuable tool for investigating ice flow dynamics, but sufficient data acquisition in remote and exposed glaciated terrain remains challenging. For data acquisition on a highly crevassed and remote outlet glacier in Greenland we developed self-sufficient and easily deployable seismic stations, "SG-boxes". The SG-boxes contain their own power supply via solar panel, a three-component omni-directional geophone and a GNSS receiver. The SG-boxes can be deployed and retrieved from a hovering helicopter, allowing for deployment in difficult terrain. To assess their performance we conducted a field test comparing the SG-boxes to established on-ice geophone installations at Gornergletscher in Switzerland. Moreover, data from a first SG-box deployment in Greenland were analyzed. The SG-boxes exhibit consistently higher noise levels relative to colocated conventional geophones and a correlation between noise levels, wind and air temperature is found. Despite their noise susceptibility, the SG-boxes detected a total of 13,114 Gornergletscher icequakes over 10 days, which is 30% of the total number of icequakes detected by conventional geophone stations. Hence, even in sub-optimal weather conditions and without additional noise reduction measures, the SG-boxes can provide unique and valuable data from challenging glaciated terrain where no conventional seismic installations are possible.

Production Editor:
Gareth Funning
Handling Editor:
Stephen Hicks
Copy & Layout Editor:
Théa Ragon

Received:
September 23, 2022
Accepted:
January 6, 2023
Published:
January 11, 2023

Non-technical summary Several glacier processes produce seismic signals: small vibrations for example caused by crevasses forming in the ice or the glacier slipping across the bed. These vibrations, called icequakes, give valuable information about glacier flow dynamics and can be measured with seismological sensors at the glacier surface. However, installing seismological sensors on crevassed, exposed and remote glaciated terrain is challenging. Therefore, creative solutions are necessary. For data acquisition on a highly crevassed and remote Greenlandic outlet glacier, we developed self-sufficient and easily deployable seismic stations, "SG-boxes". The SG-boxes receive power via a solar panel, contain a three-component seismic sensor and GNSS receiver for location logging and can be lowered and retrieved from a hovering helicopter. We assessed the SG-boxes performance by comparing them against regular seismic sensors during a 10-day field test on a Swiss glacier. In addition, we analyzed data from a first SG-box deployment in Greenland. We found that the SG-boxes have higher noise levels compared to regular sensors and are especially correlated with increased wind speeds and air temperature. Despite their noise susceptibility, the SG-boxes provide us with unique and valuable data from areas where regular sensor installations are not possible.

Introduction

In recent years glacier seismology has proven to be a valuable tool for investigating short and long term ice flow dynamics (Aster and Winberry, 2017; Podolskiy and Walter, 2016). Glacier seismology provides unique sub-surface information of ice flow and hydraulic processes at a high temporal resolution. These processes include microseismic stick-slip events and stick-slip tremor at the bed enabling us to study basal sliding which is difficult to monitor with other methods (Helmstetter et al., 2015; Röösli et al., 2016a; Guerin et al., 2021). Moreover, fracture icequakes as a result of crevasse formation provide information on stresses at and below the surface (Mikesell et al., 2012; Lindner et al., 2019), changing seismic velocities can be diagnostic for englacial damage (Walter et al., 2015; Sergeant et al., 2020; Chmiel et al., 2021) and glaciohydraulic tremors allow us to study subglacial hydrology (Bartholomaus et al., 2015; Labedz et al., 2022).

Despite the advantages, seismological measurements on glaciers and ice streams pose logistical and technical challenges, especially at remote and exposed locations such as hanging glaciers in Alpine regions (Faillettaz et al., 2015) and the polar ice sheets in Greenland and Antarctica. Areas of interest are often difficult to access, which demands more creative solutions for seismological data acquisition. Snow-free glacier regions are particularly challenging: as a result of surface melt, installing conventional seismological equipment, such as surface geophones, requires the ability and space

*Corresponding author: ana.nap@geo.uzh.ch

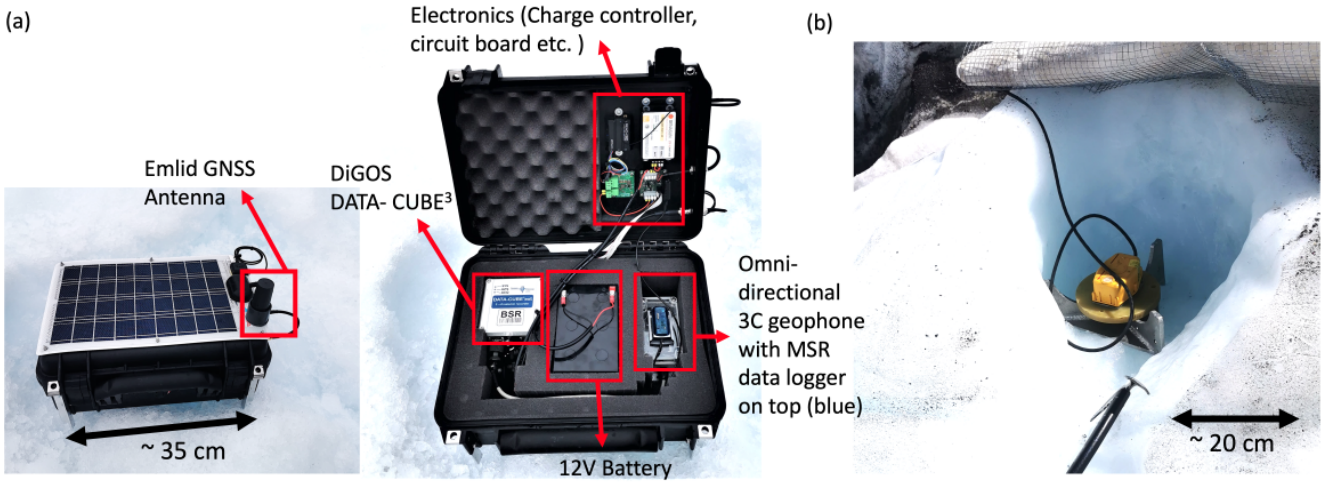

Figure 1 (a) Photos of a SG-box with closed and open lid. The SG-boxes housing is a waterproof Peli^{TM} Protector case. The SG-boxes are equipped with an Emlid Reach M2 GNSS receiver, a 14 Hz three-component omni-directional geophone (SM-6 Omni-Directional by SENSOR Nederland) and a data logger from MSR Electronics GmbH. (b) Photo of a conventional geophone station that was used as reference to compare and validate the SG-boxes. These stations are equipped with a 4.5Hz three component geophone (PE-6/B manufactured by SENSOR Nederland) placed on a metal tripod and sampled with the same type DIGOS Data-CUBE^3 as the SG-boxes.

to move around on-ground and/or the need to return every day or every couple of days to re-align the sensors to a horizontal position (Walter et al., 2008; Lindner et al., 2019). A solution to eliminating the requirement of regular maintenance is the use of borehole sensors, which do not demand maintenance visits for up to weeks or months, depending on the depth of the installation and power supply. However, borehole sensors are more costly than surface geophones, take longer to install and can be complicated or even impossible to install in highly crevassed and exposed glaciated terrain. Thus, sufficient data acquisition in these remote areas of interest demand a different approach from conventional surface geophones or borehole sensors.

Here, we present an innovative, easily deployable, self-sufficient seismic recording system designed for use on a remote and difficult to access outlet glacier in Greenland. We describe the design and evaluate the performance of these seismic boxes through a field test on Gornergletscher in Switzerland, as the extreme environment in Greenland complicates comprehensive testing. During the test at Gornergletscher, conventional geophone installations, previously used for on-ice data acquisition (Lindner et al., 2019), were installed as a base-line reference. We compare the conventional geophone data to the data acquired with the seismic boxes and we combine seismological data with weather data to show a critical relation between noise levels and wind. Despite the noise susceptibility, our portable seismic boxes provide valuable measurements in poorly accessible glaciated regions, where typical instrumentation is not possible.

Instrument Design

The main requirements for the instruments are that they are compact, self-sufficient, simple to deploy and retrieve from a hovering helicopter, require no regular maintenance and can handle tilting caused by surface melt. The outcome was the design of the ”SG-boxes”, where the ”S” stands for seismic and the ”G” for GNSS (Global Navigation Satellite System) shown in Figure 1a.

The outside case of the SG-boxes are waterproof Peli^{TM} Protector cases. The SG-boxes contain a self-assembled three-component sensor with three 14 Hz omni-directional geophones (SM-6 Omni-Directional by SENSOR Nederland) fixed directly to the bottom of the box, sampled with a DIGOS Data-CUBE^3 digitizer, as well as an Emlid Reach M2 GNSS receiver with the antenna on top of the box lid. The GNSS device is multi-channel (frequencies L1, L2 and L5) and acquires all constellations. The geophone components are placed in the transparent plastic case visible on the right side of the SG-box underneath the blue data logger from MSR Electronics GmbH, that is attached to the top of the plastic geophone case. Every 5 minutes the MSR data logger records the temperature inside the box, the battery voltage and the tilt over three axes allowing for a more detailed analysis of the box performance.

The concept is to place the box directly on top of the ice such that ground movement is conveyed to the geophone inside the box. Omni-directional geophone components are used to ensure that the data are minimally affected by tilt of the box caused by ice melt, snow drift or sliding. The omni-directional geophones are equipped with an internal rotation system that keeps the geophone component at its original orientation, even when tilted. To prevent overall sliding of the SG-boxes on a sloped surface, screw-on metal spikes are attached to the bottom of the box. The GNSS receiver measures the position of the box at 1 Hz, which is a necessity for subsequent data analysis as these boxes are designed for use on fast-flowing (up to 40 m/day) glaciated terrain in Greenland (Joughin et al., 2008). The boxes are self-sufficient in their power supply from a solar panel

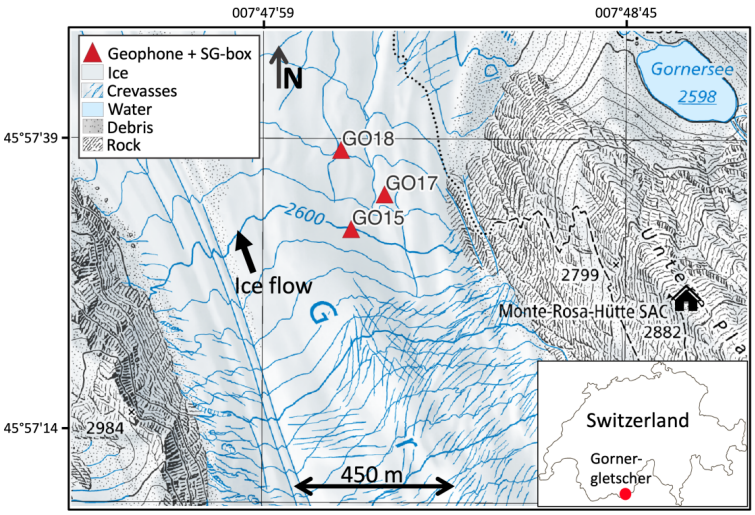

Figure 2 Overview of study site and sensor locations. The red triangles show the sensor locations where regular geophones and SG-boxes were co-located at a maximum of two meters from each other. (Source map: Swisstopo, Swiss Federal Office of Topography). Bottom right corner: Location of test site in Switzerland.

fixed on the box lid and are equipped with a charge control unit which prevents complete drainage of the battery in case of sustained time periods without sufficient solar energy. The SG-boxes can be lowered and recovered from a hovering or touched-down helicopter, either with a rope or by hand, depending on how close the helicopter can approach the surface. Lowering and retrieving the SG-boxes from a hovering helicopter by rope can be achieved by attaching a hook or anchor on a rope to suspension system of wires attached to the top of the box. This suspension system is not shown in Figure 1a, but was tested successfully.

Field test at Gornergletscher

Since extreme polar conditions and poor site access hampered detailed testing in Greenland, we first performed a field test at Gornergletscher in Switzerland in 2021 from the 29th of June until the 15th of July. This allowed us to gain extensive insight into the performance of the SG-boxes via a comparison between data from established installation techniques for on-ice deployment and the SG-boxes. For the validation and comparison of the SG-box data we used three-component geophone stations as shown in Figure 1b. These are 4.5Hz, three-component geophones (PE-6/B manufactured by SENSOR Nederland) previously used in glacier seismology research by Lindner et al. (2019) and sampled with DIGOS Data-CUBE^3 digitizers as well, the same digitizer as in the SG-boxes. The regular geophones (Fig. 1b) are henceforth referred to as geophone(s).

The test deployment consisted of an array of 3 geophones arranged with inter station distances of 130-215 m (Fig. 2). As done in previous field campaigns, the geophones were placed in a pit dug into the ice with one melt-water drainage channel and covered with a white fleece tarpaulin to reduce ablation (Figure 1b). These geophone stations require daily or bi-daily additional digging of the pit and re-levelling of the sensors to account for surface melt. The geophones were co-located with an SG-box (red triangles in Fig. 2), which were placed 1-2 m from the geophone at the ice surface. At GO15 and GO18 the geophones and SG-boxes were co-located for the entire test period and at GO17 only for a total of 10 days. The station names of the geophones are GO15GP, GO17GP and GO18GP and for the SG-boxes GO15SG, GO17SG and GO18SG, respectively. There are no data gaps on any of the stations except for some small (<20 minutes) data gaps in the geophone data during maintenance visits (e.g. changing of batteries or downloading data).

SG-box performance

In the results we focus on the seismological performance of the SG-boxes compared to regular geophones. The GNSS aspect of the SG-boxes to measure glacier flow velocities is of equal value to our research, but the performance of the Emlid GNSS/GPS receivers is already well established and does not need extensive additional analysis. For the sake of giving a complete overview of the SG-boxes performance, information on the GNSS processing and resulting flow speeds is included in the Supplementary Material S1.

Noise characteristics

A main limit on the performance of seismic sensors is (environmental) background noise (McNamara and Buland, 2004). If background noise exceeds or approaches the amplitude of the target signal, data usefulness becomes compromised. Seismic data from high-melt ablation zones contain a wealth of potential noise sources, such as melt-water flow and moulin drainage (Röösli et al., 2016a), rock/ice fall activity (Guillemot et al., 2020), wind (Frankinet et al., 2021; Winter et al., 2021), ice fracturing (Podolskiy and Walter, 2016) and in case of more populated areas also anthropogenic noise (Larose et al., 2015). Given the close proximity of co-located SG-boxes and geophones, we assume that both

sensor types record the same noise signals allowing comparison of their continuous records to evaluate the installation quality. As a result of the manner of installation of the SG-boxes (i.e. loosely placed on the ice surface) we expect them to be particularly sensitive to wind noise and we anticipate a reduced level of ground coupling compared to the geophones.

Probabilistic power spectral density (PPSD)

To estimate noise levels across a range of frequencies we computed PPSDs for both the SG-box and geophone at each station with the ObsPy package (Beyreuther et al., 2010) according to McNamara and Buland (2004). Figure 3a/b display PPSD plots for GO15SG and GO15GP, respectively, and Figure 3c shows the mean PPSD for each sensor.

Across all frequencies the SG-box PPSD in Figure 3a shows a larger variance as well as higher amplitudes than the geophone. The different bands in the PPSD in Figure 3a indicate that noise levels in the SG-box data fluctuate more over time than those of the geophone data. In Figure 3c we see that the mean PPSDs of the SG-boxes are at least 10 dB above the geophones for frequencies up to 50 Hz and up to 20 dB higher for frequencies above 100 Hz.

Background noise, wind and air temperature

A first look at the time series data and spectrograms of the SG-boxes shows that elevated noise levels occur in bounded time periods. During these periods the noise levels of the SG-boxes are up to 40 dB higher than the noise levels of the geophones (Fig. 4). In summer, glacial seismic data often experience heightened noise levels during the day as afternoon air temperatures boost meltwater flow (Canassy et al., 2012; Podolskiy and Walter, 2016; Röösli et al., 2016a; Aster and Winberry, 2017). However, this type of noise usually follows a diurnal rhythm which was not the case for the elevated noise periods of the SG-boxes. In contrast, we found a correlation between the SG-box noise levels and wind speed data from a nearby MeteoSwiss weather station. Considering that the SG-boxes are deployed at the ice surface and the geophones are inside a pit in the ice (Fig. 1) it is consequential that the geophones are more protected against strong winds. A comparison between SG-box data and geophone data during periods of low to no wind (hourly average <5 km/h) and strong wind (hourly average >20 km/h with gusts up to 60 km/h) is shown in Figure 4. During a period of no wind the SG-boxes and geophones contain comparable noise levels and display matching waveform data (Figs. 4a and 4b). For periods with strong wind, where the hourly average is 20 km/h, the SG-boxes experience up to 40 dB higher noise levels compared to no wind (Figs. 4c and 4d). The geophones experience elevated noise levels as well, but only by up to 10 dB.

To quantify and assess temporal variations in noise levels, we computed spectrograms for both the geophones and the SG-boxes across the full test period. The spectrograms were computed in 5.12 s windows with 50% overlap. From the spectrograms we computed 60

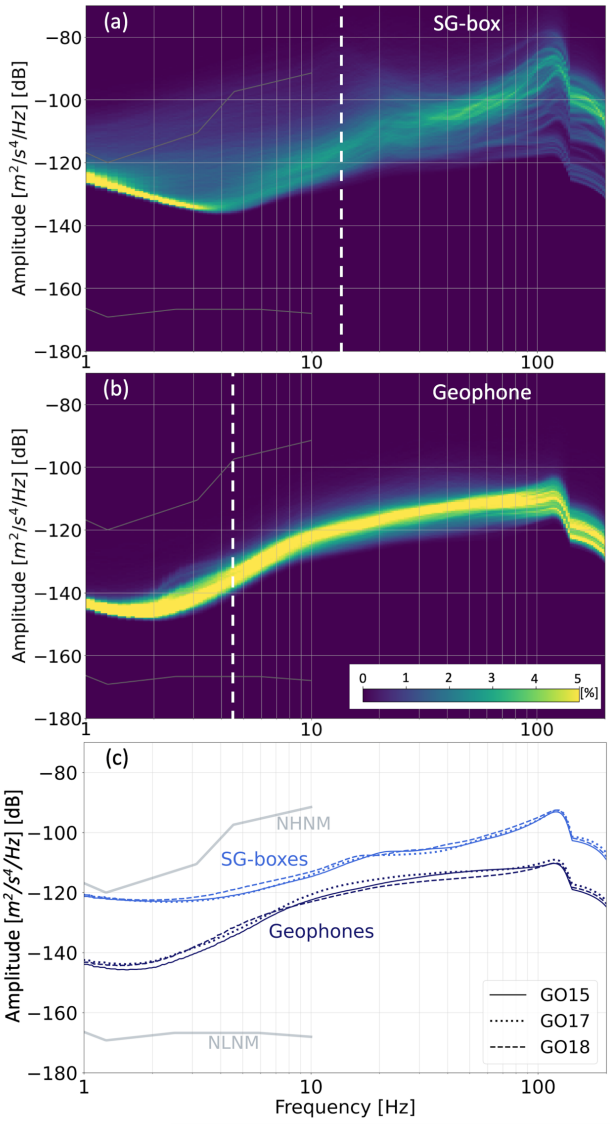

Figure 3 Probabilistic power spectral density (PPSD) of the vertical component at station GO15 for the entire 15 day test period (computed with the ObsPy package (Beyreuther et al., 2010) according to McNamara and Buland (2004)). Grey lines mark the low and high noise models (NLNM and NHNM according to Peterson (1993)) and the vertical white dashed lines indicate the natural frequency of the sensor, 4.5 Hz for the geophones an 14 Hz for the SG-boxes. (a) PPSD GO15SG (b) PPSD GO15GP. (c) Mean PPSD values for all stations (GO15, GO17 and GO18).

minute average power spectral density (PSD) windows in different frequency ranges, 14-30 Hz, 30-100 Hz and 100-190 Hz. Through dividing the average PSDs of the SG-boxes by those of the geophones we obtain a ratio that expresses the noise level of the SG-boxes relative to the geophones for each frequency window. For station GO15 the results of these computations are displayed in Figure 5a and Figure 5b. For station GO17 and GO18 the same results can be found in Fig. S2 and S3. Note that most peaks in Figure 5a and Figure 5b occur during geophone maintenance visits, indicated by the red arrows. When performing maintenance on the stations the sensors were occasionally moved and the pits of the geophones were deepened using an ice-axe, causing

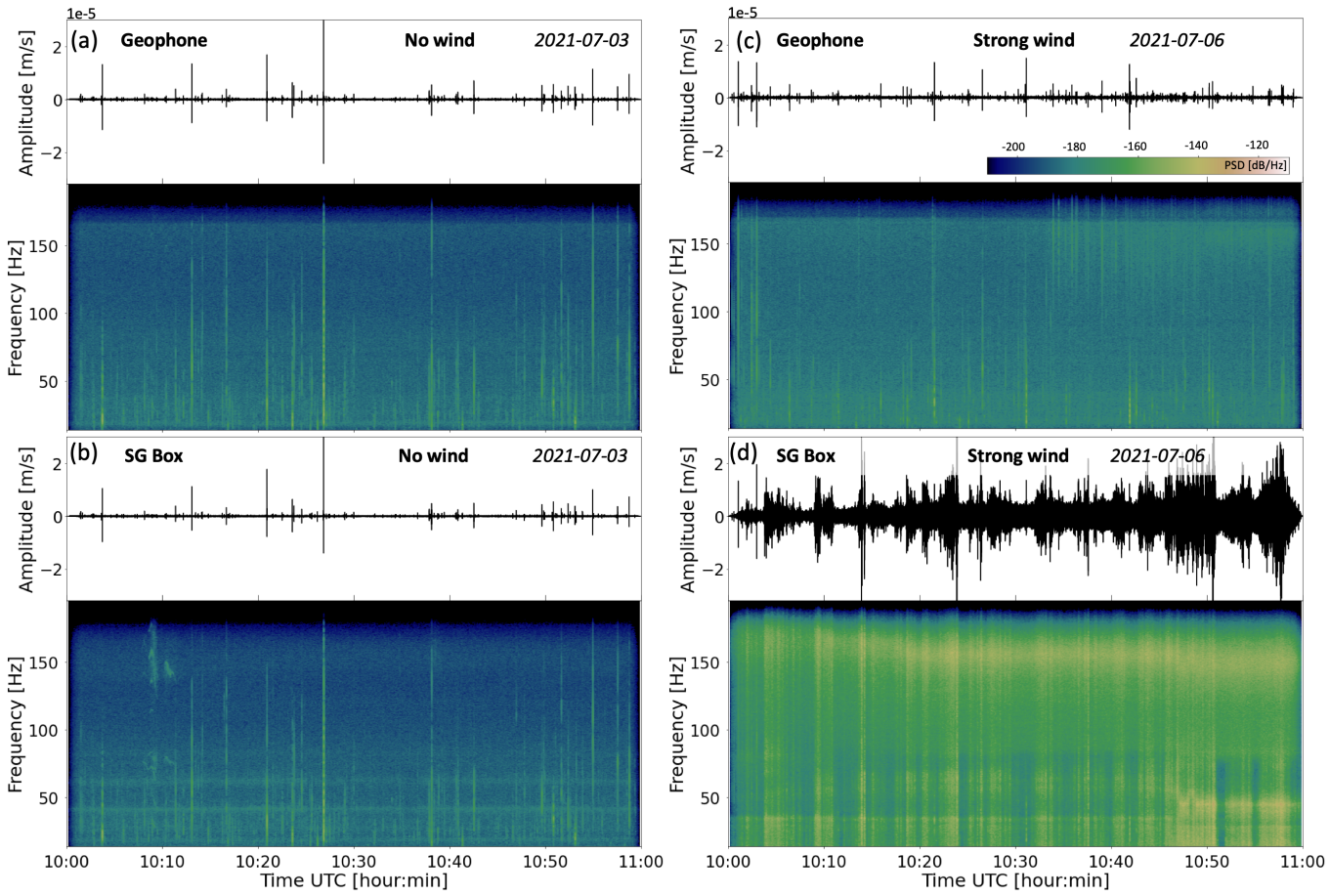

Figure 4 Waveform data and respective spectrograms for times with no wind on July 3rd 2021 (hourly average <5 km/h) and times with strong wind on July 6th 2021 (hourly average >20 km/h with gusts up to 60 km/h) from station GO15. (a) GO15GP data with no wind. (b) GO15SG data with no wind. (c) GO15GP data during strong wind. (d) GO15SG data during strong wind.

high, short duration (<10 minutes) peaks of energy in the data.

Figures 5a/b show that for 70% of the test period the noise level of the SG-box lies above that of the geophone. The high frequency window of 100-190 Hz generally exhibits the highest ratio, a characteristic that can also be seen in the spectogram of Figure 4d. Figure 5b shows that noise levels can be identical for the SG-box during periods of low wind speed (<5 km/h). Periods of strong wind (hourly average >20km/h and gusts up to 80 km/h) consistently correlate with periods that show elevated noise levels. However, the opposite does not apply: periods of little to no wind do not always correspond to a ratio of one in Figure 5b. For some elevated noise periods during low wind, such as on the 5^{th} and 11^{th} of July, a correlation between elevated noise levels and higher (> 7.5 °C) air temperature can be identified. The above mentioned correlations for station GO15 also apply to stations GO17 and GO18 (Fig. S2 and S3 in the Supplementary Material).

Generally, seismic energy caused by glaciohydraulic processes and surface meltwater flow is concentrated at frequencies below 35 Hz (Bartholomaus et al., 2015; Podolskiy and Walter, 2016; Röösli et al., 2016b; Labedz et al., 2022) and is therefore not likely to explain the periods of high frequency noise (>100 Hz) during periods with low wind speeds and high air temperature such as at the start and end of the test period. We also have to consider that the weather data originates from a weather station next to the Monte Rosa Hut, which is 850 m from the deployment and at 450 m higher elevation. Therefore, the wind speed data might not fully represent the situation at the glacier and thus at the sensors. Low wind speeds could be measured at the weather station while strong wind occurred at the glacier, either because of catabatic winds or a more sheltered position of the hut with certain wind directions. We also checked tilt of the SG-box as a possible explanation for elevated noise levels. Figure 5c, displays the tilt of the SG-box on the X, Y and Z component as measured every five minutes by the MSR data logger (see Fig. 1 for the details of the SG-box). The tilt data from Figure 5c shows no correlation with sustained periods of elevated noise for the SG-box as displayed in Figure 5a/b. Only peaks correspond to the moment of changing tilt (e.g. sliding down icy slope). These tilt events account for the peaks in the average PSD that are not caused by maintenance visits.

Waveform quality

Although the noise levels show no correlation with tilt, the waveform quality of the SG-boxes could still be affected. The seismic sensors used for the SG-box are

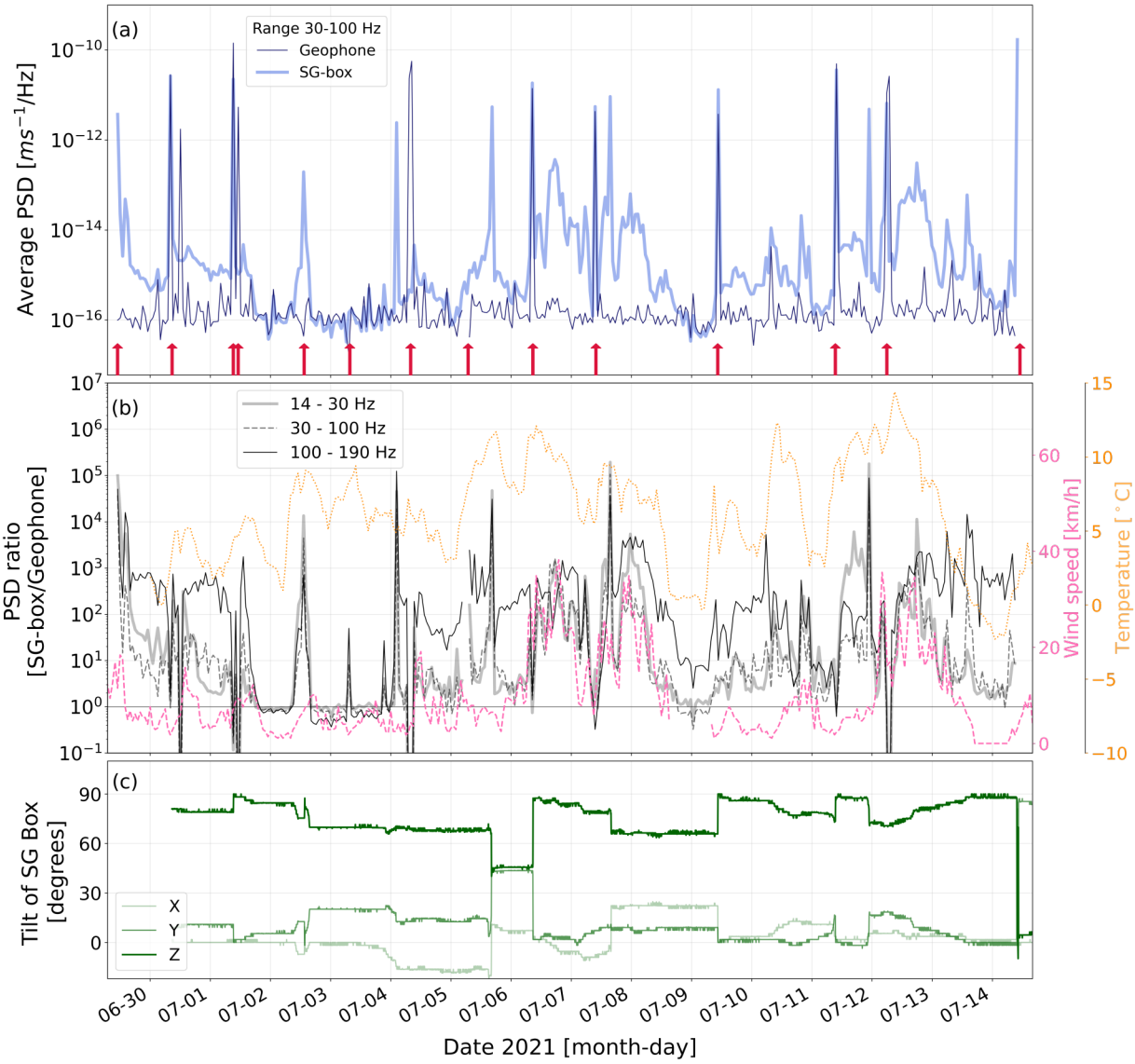

Figure 5 Noise levels and tilt time series of Station GO15. (a) Average power spectral density (PSD) of the SG-box and geophone in a frequency range of 30 to 100 Hz. The average PSD is computed by taking the average value of 60 minute windows in the spectrogram for a defined frequency range. The red arrows indicate the maintenance visit times at the stations. (b) Ratio between average PSD of SG-box and geophone in three frequency windows: 14-30 Hz, 30-100 Hz and 100-190 Hz. Hourly averaged wind speed and hourly averaged temperature measured at the MeteoSwiss weather station at the Monte Rosa Hut are displayed in dashed pink and dotted orange, respectively. A ratio of 1 (i.e. 10^0) corresponds to equal PSD levels of SG-box and geophone. (c) Tilt of three axis of the SG-box measured every 5 minutes by the MSR data logger accelerometer. The SG-box is exactly horizontal when X, Y and Z are 0, 0 and 90 degrees, respectively.

omni-directional, but it remains to be shown if tilting the SG-box from a horizontal position will affect the data quality. Figure 5 shows that prolonged periods of tilt from a horizontal position do not correlate with heightened noise levels of the SG-box. Other than increased noise, reduced waveform accuracy because of tilting is a known problem for seismological sensors in general (Ringler et al., 2015; Faber and Maxwell, 1997). Also coupling and general data fidelity could be affected by sliding of the SG-box.

During the test period, GO15SG experienced an extended period of tilt beyond 45 degrees. This "tilt event" occurred around 16:00 UTC on the 5^{th} of July and the SG-box was re-levelled during a maintenance visit at 9:00 UTC on the 6^{th} of July. The tilt data measured by the MSR data logger can be found in Figure 5c. Figure 6e shows a photo of the tilted position of the SG-box during the "tilt-event" (taken during the maintenance visit before levelling the SG-box). To assess waveform quality, we cross-checked the waveforms of the SG-box and the geophone for different icequake events before, during and after the "tilt event". In Figure 6 the waveforms of the vertical component for four selected events are found. Identical figures as Figure 6 for the horizontal components are in Fig. S4 and S5.

The waveforms of the SG-box closely resemble those of the geophone, before, during and after the SG-box is tilted (Fig. 6). In the waveform time series a slight difference can be found in the amplitudes of the SG-box and geophone. We assume this difference is caused by

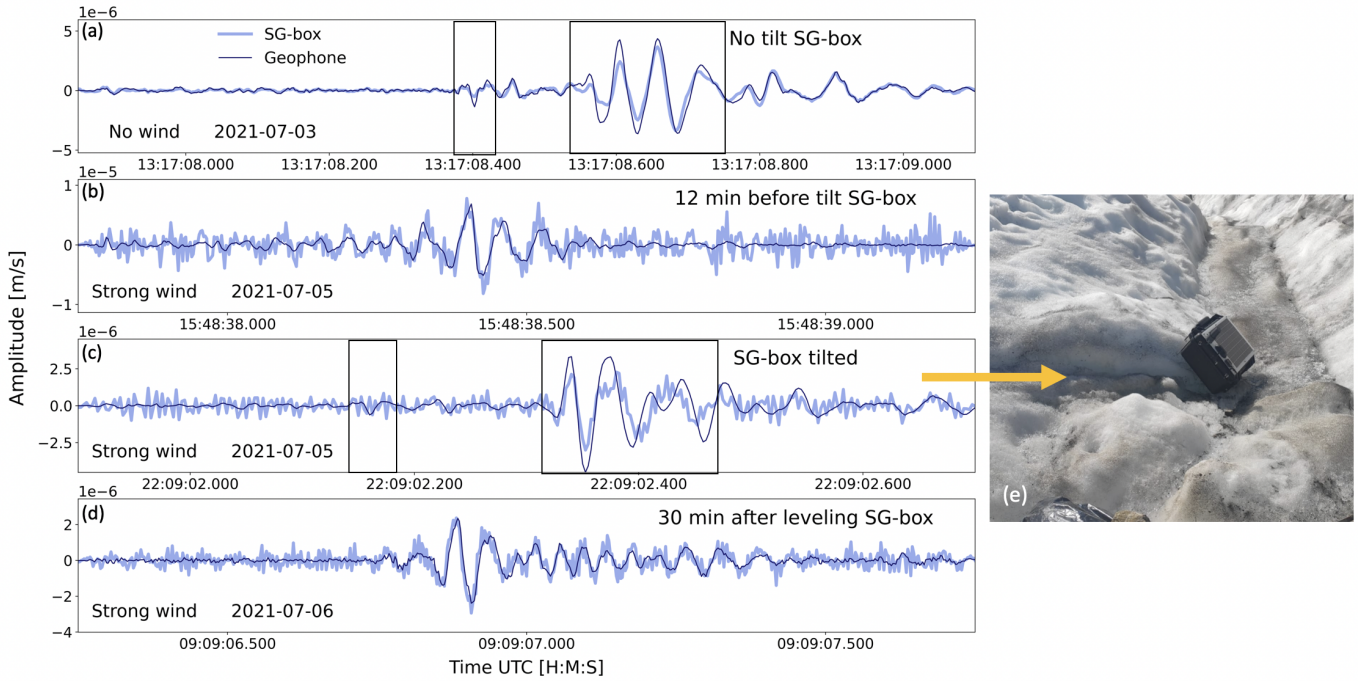

Figure 6 Example of match between SG-box and geophone for selected icequake events before, during and after extreme tilt of SG-box at station GO15. Here the vertical component is shown and the data are bandpass filtered between 14 and 190 Hz. The tilt occurred between approximately 16:00UTC on 2021-07-05 and 09:00UTC the next day. The measured tilt can be found in figure 5. (a) No tilt on 2021-07-03 with no wind. (b) 12 minutes before tilt occurred on 2021-07-05. (c) During tilt of SG-box on 2021-07-05. The amount of tilt the SG-box experienced can be seen in (e), the picture is taken in a horizontal position. (d) 30 minutes after placing the SG-box in a horizontal position again.

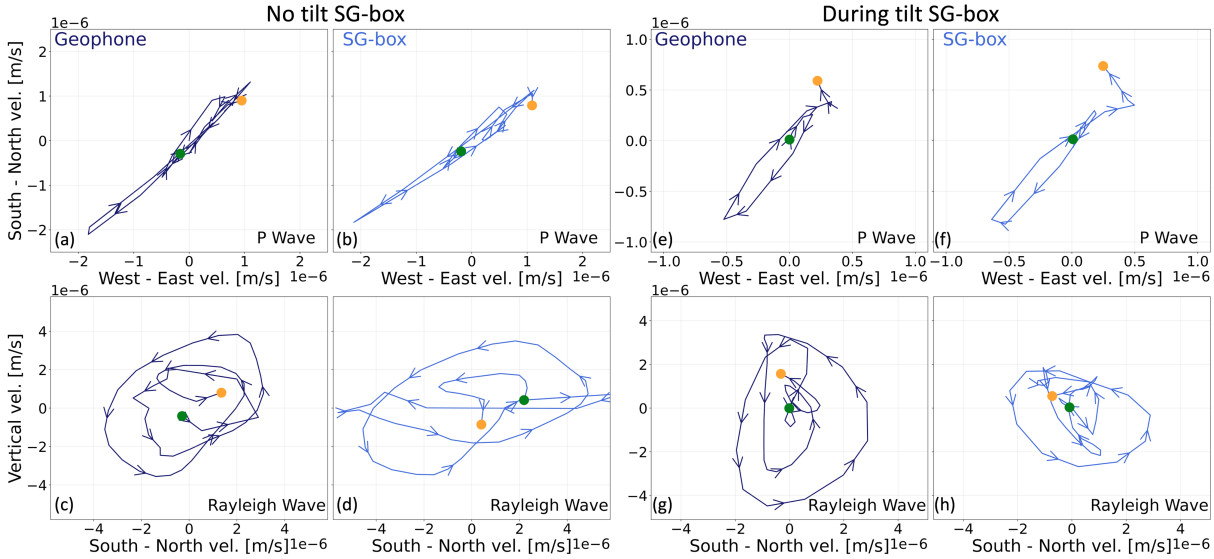

Figure 7 Particle motion of selected events in Fig. 6a and 6c. Green points mark the start of the motion and orange points mark the end. (a, b, c, d) Particle motion in m/s of event depicted in Fig. 6a for the geophone (a and c, dark blue) and SG-box (b and d, light blue) when the SG-box was not tilted. The data are bandpass filtered between 14-150 Hz. The P-wave (a and b) and Rayleigh wave (c and d) correspond to the first and second outlined box in Fig. 6a respectively. (e, f, g, h) Particle motion in m/s of event depicted in Fig. 6c for the geophone (e and g) and SG-box (f and h) when the SG-box was tilted as shown in Fig. 6e. The data are bandpass filtered between 14-100 Hz. The P-wave (e and f) and Rayleigh wave (g and h) correspond to the first and second outlined box in Fig. 6c respectively.

the fact that they are different sensor types and because of a difference in coupling, as the SG-boxes are more loosely placed on the ice than the geophones. Further, a distinct difference between the waveforms of Figure 6b, 6c and 6d is the presence of high frequency noise in the SG-box data, likely caused by elevated wind speeds during those times (Fig. 4 and 5). The absence of high frequency noise in Figure 6a, when there was low to no wind, supports this assertion. In general, the vertical components are more affected by the high frequency

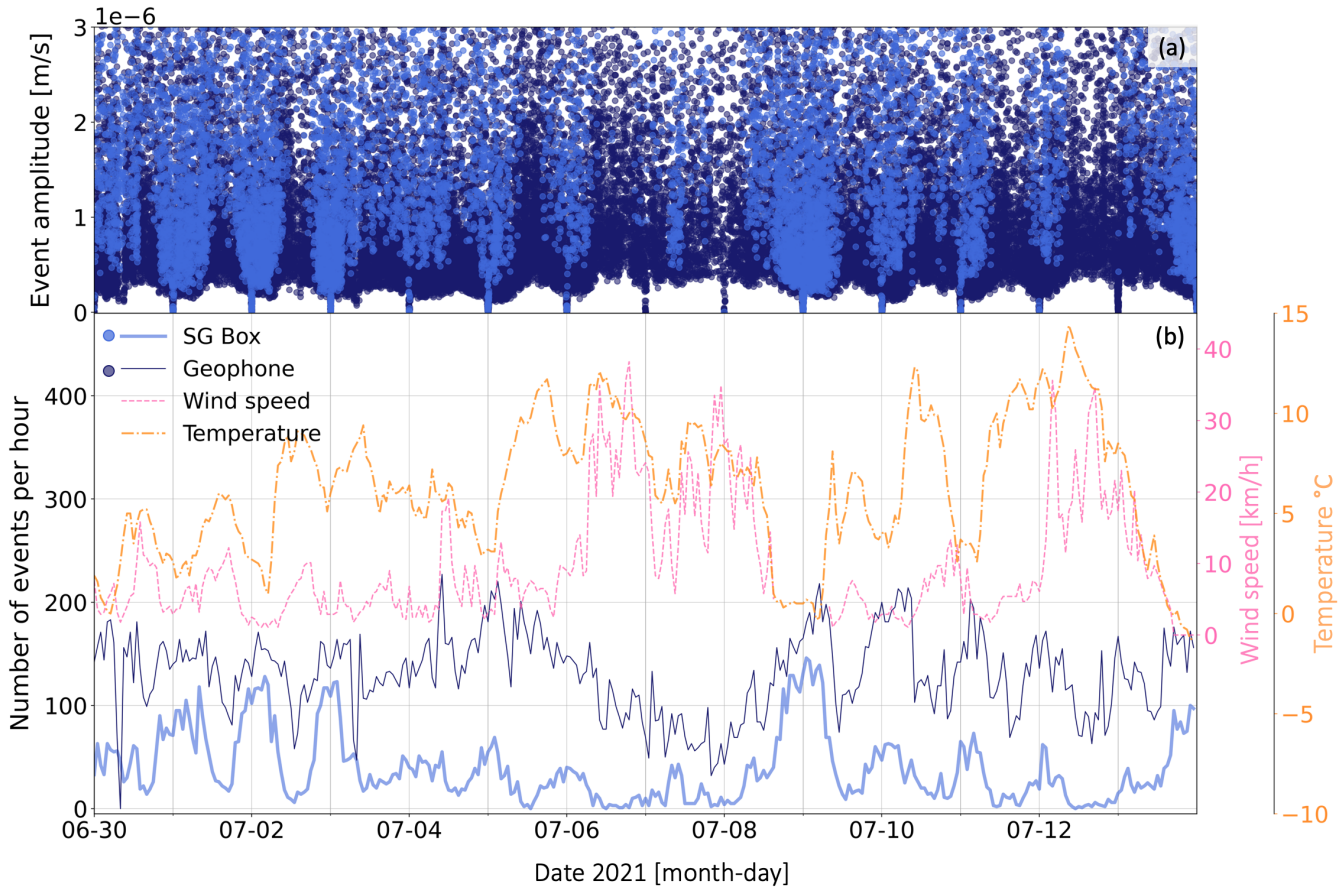

Figure 8 (a) Amplitude of each detected icequake of the SG-boxes (light blue) and geophones (dark blue). The 25% highest amplitudes are left out for clarity. Bottom: Hourly icequake detection with wind speed (dashed pink) and temperature (dotted yellow).(b) Time history of temperature, wind and hourly icequake detections for both the geophones (striped dark blue) and the SG-boxes (solid light blue).

noise than the horizontal components (see Fig. S4 and S5 in the Supplementary Material).

To further assess the quality of the waveform recordings of the SG-box before and during the tilt event we looked at the particle motion of the icequake events from Figure 6a and 6c. These selected events are assumed to be (near) surface events caused by crevasse formation or extension, as they contain clear low frequency (10-50 Hz) Rayleigh waves, compressive P-wave polarity and an estimated back-azimuth towards the S-SW where a large number of crevasses are concentrated (see Fig. 2). Figure 7a - 7d and Figure 7e - 7h show the particle motion for the P- and Rayleigh wave of the events in Figure 6a and 6c respectively. For Figure 7a - 7d the data are bandpass filtered between 14 and 150 Hz and for Figure 7e - 7h between 14 and 100 Hz, to account for the high frequency noise (Fig. 6c) that otherwise superimposes the particle motion. Both events show clear compressional motion in the horizontal plane for the P-waves and retrograde motion in the north-south oriented vertical plane for the Rayleigh waves. Figure 7 shows that even when the SG-box is severely tilted the omni-directional geophones still record the waveforms with good quality.

Event detection

To asses the useful data return further, we compared the SG-boxes and the geophones in terms of icequake event detection. For this comparison the three SG-boxes and the three co-located geophones are treated as two separate triangular arrays.

For icequake event detection we used a classic coincidence short-term/long-term (STA/LTA) trigger from the ObsPy library (Beyreuther et al., 2010) with a coincidence criterion of two out of three sensors. The STA/LTA was performed only on the vertical components that were filtered between 14 and 100 Hz. The STA window was set at 0.1 s and the LTA window at 20 s, the windows were determined in an empirical manner. The algorithm was run separately for the three SG-boxes and the three geophones. To eliminate false picks we performed cross-correlations between the stations within an array when a detection was triggered. By trial-and-error we determined a cross-correlation threshold of 0.5 for an event to be kept. For the geophones this resulted in 44,100 events out of 70,358 that were kept after cross-correlation confirmation and 13,114 out of 47,233 for the SG-boxes. This testifies to a larger number of false detections for the SG-boxes, which is expected considering the fluctuating noise levels which complicate accurate picking with a STA/LTA algorithm. The settings of the cross-correlation threshold also delete a minority of

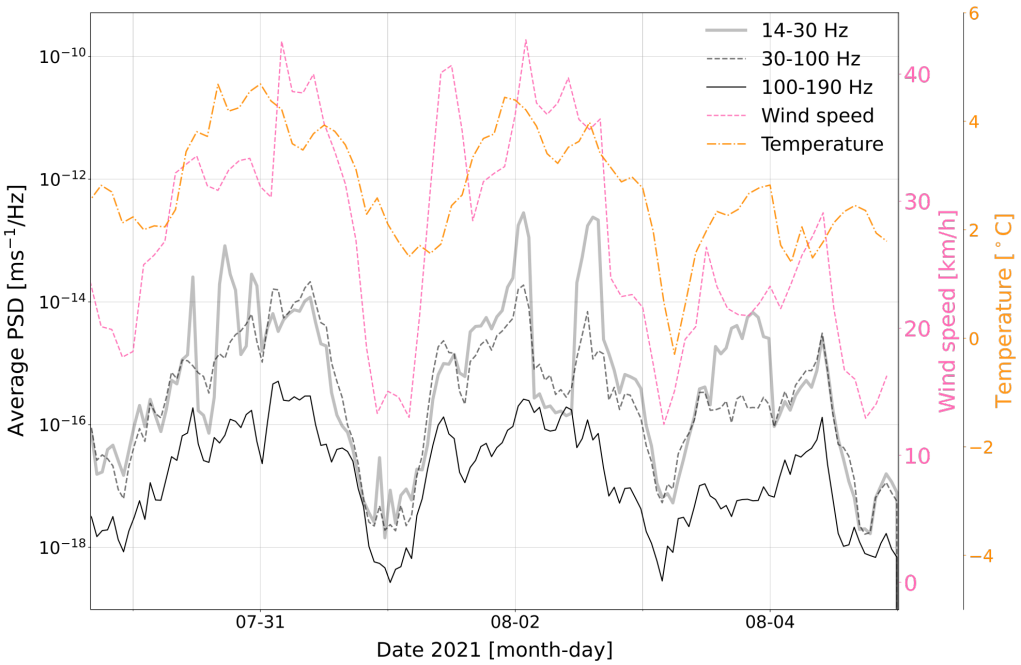

Figure 9 Average PSD of SG-box (grey) installed on Sermeq Kujalleq in Greenland in three frequency windows, 14-30 Hz, 30-100 Hz and 100-190 Hz. Average air temperature and average wind speed (2 hour window averages are transmitted via satellite connection) are plotted on top in dotted orange and striped pink, respectively.

positive picks, but from visual confirmation completely eliminate false positives, which is important for a valid instrument comparison. False positive picks in the SG-box data mainly concentrate in large amplitude noise bursts between 10 s - 10 min in length, where consecutively tens of picks were placed by the STA/LTA algorithm without an actual event being present.

The results show that the geophones consistently detect more events per hour than the SG-boxes (Fig. 8). Specifically, around 30% of events detected on the geophones were detected on the SG-boxes. This is expected considering the elevated noise levels of the SG-boxes compared to the geophones. Additionally, a clear diurnal cycle exists for the detectability of weaker events (Fig. 8). This phenomenon has been described by Walter et al. (2008); Canassy et al. (2012) and Röösli et al. (2014), who linked daily changes in amplitudes of the weakest detectable events to melt-induced seismic background noise, primarily driven by glaciohydraulic tremor. In our study, both wind speed and air temperature show a link to the number of detected events (Fig. 8). Temperatures above 5 $°C$ and wind speeds above 20 km/h correspond to substantially lower numbers of detected events, especially for the SG-boxes.

Discussion

Compared to the conventional geophones, the SG-boxes are more affected by environmental noise such as wind and air temperature. Nevertheless, the omnidirectional sensors within the SG-box eliminated the effect of tilt on data quality and icequake waveforms show good correlation with geophone records even when the SG-box is tilted beyond 45 degrees from a horizontal position. During the test period at Gornergletscher the SG-boxes were able to detect a total of 13,114 icequakes compared to 44,100 detected by the geophones (i.e. 30%).

Our findings that seismic background noise in SG-box data correlates with wind and air temperature (i.e. increased meltwater flow) are supported by data from a first acquisition with SG-boxes on Sermeq Kujalleq in Kangia (also known as Jakobshavn Isbræ), an outlet glacier on the west coast of Greenland. The boxes were specifically designed for data acquisition on this glacier, as the fast flowing trunk of Sermeq Kujalleq is difficult to access. The first 15 km are extremely crevassed so landing by helicopter is not possible, in the best case a touchdown can be performed, where the helicopter lands lightly on the ice surface but does not turn off the engine. Therefore, regular seismological equipment cannot be installed.

In July/August 2021, six singular SG-boxes at an intersensor distance of approximately 5 km were deployed along the fast ice stream of Sermeq Kujalleq. A deployment map of these SG-boxes and GNSS flow velocity data from two SG-boxes can be found in the Supplementary Material S4. As the SG-boxes were just singular sensor deployments at a relatively large distance from each other, we could not perform the same type of analysis we did for the data from Gornergletscher. Nevertheless, one of the SG-boxes in this deployment was located at 20 m from a weather station, allowing us to compare temperature and wind data to the average PSD of the SG-box, similar to the comparison in Figure 5.

Figure 9 shows a clear correlation between the average PSD and wind and temperature, with average wind speeds above 25 km/h and temperatures above 2 $°C$ corresponding to up to four orders of magnitude higher av-

erage PSD levels. The main difference between the data from Greenland and the data from Gornergletscher is that in Figure 9 the low frequency window (i.e., 14-30 Hz) is consistently higher than the other two frequency windows. An explanation for this could be that the SG-box in Greenland was located close to a sub-glacial or englacial water channel or moulin that would dominate on-ice noise in this frequencies range (Bartholomaus et al., 2015; Röösli et al., 2016b; Köpfli et al., 2022; Labedz et al., 2022). The hydrological system on the Greenland icesheet is of a different scale than at an Alpine glacier, such as Gornergletscher. Considering the size of the englacial and subglacial water channels and moulins, it is not unexpected that different frequencies dominate the overall seismic energy (Röösli et al., 2016b; Podolskiy, 2020).

The fact that the SG-boxes experience higher levels of background noise and are more sensitive to wind than the geophones is not surprising given the manner of deployment: on top of the glacier surface instead of the more protected deployment used for the geophones (Fig. 1). Although the SG-box deployment results in higher noise susceptibility and a reduced level of coupling, the SG-boxes have the advantage of reduced maintenance as well as simple deployment and retrieval. They are suitable for use in remote and exposed areas where deployment of typical instrumentation, such as regular geophones or borehole seismometers, is not possible. The SG-boxes provide unique access to valuable data from these areas. Further, additional measures can be taken to maximize useful data return like placing the SG-boxes in an array to allow for array processing and other advanced filtering techniques to reduce background noise that is uncorrelated between individual stations (Gibbons and Ringdal, 2006; Seydoux et al., 2016).

Summary and Conclusion

We have studied the performance of self-sufficient and easily deployable seismic stations (SG-boxes) for use in remote and hard-to-access glaciated regions such as a highly crevassed outlet glacier in Greenland. By comparing the SG-boxes to regular geophones through a field test at Gornergletscher, Switzerland, we assessed the performance of the boxes. Also, data from a first acquisition with an SG-box in Greenland were analysed. The results from both deployments show that the SG-boxes experience elevated noise levels compared to the regular geophones, especially in the lower frequency range of 14-30 Hz and the higher frequency range of 100-190 Hz. As a clear correlation is found between SG-box noise levels and wind and air temperature data, elevated noise levels are most likely caused by the exposure of the boxes on the glacier surface, in contrast to the more protected deployment of the geophones. Future investigations will benefit from placing the boxes into arrays that allow for array processing to reduce noise and increase signal return. Despite their noise susceptibility, the SG-boxes detected 30% of icequake events compared to conventional geophone installations during a 10 day test period with variable weather. Hence, even in sub-optimal weather conditions and without additional noise reduction measures the SG-boxes can provide unique and valuable data from poorly accessible glaciated terrain.

Acknowledgements

We want to thank the reviewers for taking the necessary time and effort to review the manuscript. We sincerely appreciate all your valuable comments and suggestions, which helped us in improving the quality of the manuscript. We thank D. Wasser for his expert knowledge and help with designing, building and testing the technical side of the SG-boxes. This research has been supported by the Schweizerischer Nationalfonds zur Förderung der Wissenschaftlichen Forschung grant no. 200020_197015.

Data availability

All data are available at the following link: https://zenodo.org/record/7516192.Y7wjsSwo9z1 with doi:10.5281/zenodo.7516192.

Competing interests

All authors declare that they have no conflicts of interest.

References

Aster, R. C. and Winberry, J. P. Glacial seismology. *Reports on Progress in Physics*, 80(12):126801, Nov. 2017. doi: 10.1088/1361-6633/aa8473.

Bartholomaus, T. C., Amundson, J. M., Walter, J. I., O'Neel, S., West, M. E., and Larsen, C. F. Subglacial discharge at tidewater glaciers revealed by seismic tremor. *Geophysical Research Letters*, 42(15):6391–6398, 2015. doi: https://doi.org/10.1002/2015GL064590.

Beyreuther, M., Barsch, R., Krischer, L., Megies, T., Behr, Y., and Wassermann, J. ObsPy: A Python toolbox for seismology. *Seismological Research Letters*, 81(3):530–533, 2010. doi: 10.1785/gssrl.81.3.530.

Canassy, P. D., Faillettaz, J., Walter, F., and Huss, M. Seismic activity and surface motion of a steep temperate glacier: a study on Triftgletscher, Switzerland. *Journal of Glaciology*, 58(209):513–528, 2012. doi: 10.3189/2012JoG11J104.

Chmiel, M., Walter, F., Preiswerk, L., Funk, M., Meier, L., and Brenguier, F. Hanging glacier monitoring with icequake repeaters and seismic coda wave interferometry: a case study of the Eiger hanging glacier. *Natural Hazards and Earth System Sciences*, Sept. 2021. doi: 10.5194/nhess-2021-205.

Faber, K. and Maxwell, P. W. Geophone spurious frequency: what is it and how does it affect seismic data quality. *Can. J. Explor. Geophys*, 33(1-2):46–54, 1997.

Faillettaz, J., Funk, M., and Vincent, C. Avalanching glacier instabilities: Review on processes and early warning perspectives. *Reviews of Geophysics*, 53(2):203–224, 2015. doi: https://doi.org/10.1002/2014RG000466.

Frankinet, B., Lecocq, T., and Camelbeeck, T. Wind-induced seismic noise at the Princess Elisabeth Antarctica Station. *The Cryosphere*, 15(10):5007–5016, Oct. 2021. doi: 10.5194/tc-15-5007-2021.

Gibbons, S. J. and Ringdal, F. The detection of low magnitude seismic events using array-based waveform correlation. *Geophysical Journal International*, 165(1):149–166, Apr. 2006. doi: 10.1111/j.1365-246X.2006.02865.x.

Guerin, G., Mordret, A., Rivet, D., Lipovsky, B. P., and Minchew, B. M. Frictional Origin of Slip Events of the Whillans Ice Stream, Antarctica. *Geophysical Research Letters*, 48(11): e2021GL092950, 2021. doi: 10.1029/2021GL092950.

Guillemot, A., Helmstetter, A., Larose, É., Baillet, L., Garambois, S., Mayoraz, R., and Delaloye, R. Seismic monitoring in the Gugla rock glacier (Switzerland): ambient noise correlation, microseismicity and modelling. *Geophysical Journal International*, 221(3):1719–1735, 2020. doi: 10.1093/gji/ggaa097.

Helmstetter, A., Nicolas, B., Comon, P., and Gay, M. Basal icequakes recorded beneath an Alpine glacier (Glacier d'Argentière, Mont Blanc, France): Evidence for stick-slip motion? *Journal of Geophysical Research: Earth Surface*, 120(3):379–401, 2015. doi: https://doi.org/10.1002/2014JF003288.

Joughin, I., Howat, I. M., Fahnestock, M., Smith, B., Krabill, W., Alley, R. B., Stern, H., and Truffer, M. Continued evolution of Jakobshavn Isbrae following its rapid speedup. *Journal of Geophysical Research: Earth Surface*, 113(F4), 2008. doi: https://doi.org/10.1029/2008JF001023.

Köpfli, M., Gräff, D., Lipovsky, B. P., Selvadurai, P. A., Farinotti, D., and Walter, F. Hydraulic Conditions for Stick-Slip Tremor Beneath an Alpine Glacier. *Geophysical Research Letters*, 49(21):e2022GL100286, 2022. doi: https://doi.org/10.1029/2022GL100286.

Labedz, C. R., Bartholomaus, T. C., Amundson, J. M., Gimbert, F., Karplus, M. S., Tsai, V. C., and Veitch, S. A. Seismic mapping of subglacial hydrology reveals previously undetected pressurization event. *Journal of Geophysical Research: Earth Surface*, Feb. 2022. doi: 10.1029/2021JF006406.

Larose, E., Carrière, S., Voisin, C., Bottelin, P., Baillet, L., Guéguen, P., Walter, F., Jongmans, D., Guillier, B., Garambois, S., et al. Environmental seismology: What can we learn on earth surface processes with ambient noise? *Journal of Applied Geophysics*, 116:62–74, 2015. doi: 10.1016/j.jappgeo.2015.02.001.

Lindner, F., Laske, G., Walter, F., and Doran, A. K. Crevasse-induced Rayleigh-wave azimuthal anisotropy on Glacier de la Plaine Morte, Switzerland. *Annals of Glaciology*, 60(79):96–111, Sept. 2019. doi: 10.1017/aog.2018.25.

McNamara, D. E. and Buland, R. P. Ambient Noise Levels in the Continental United States. *Bulletin of the Seismological Society of America*, 94(4):1517–1527, Aug. 2004. doi: 10.1785/012003001.

Mikesell, T., van Wijk, K., Haney, M. M., Bradford, J. H., Marshall, H.-P., and Harper, J. T. Monitoring glacier surface seismicity in time and space using Rayleigh waves. *Journal of Geophysical Research: Earth Surface*, 117(F2), 2012. doi: 10.1029/2011JF002259.

Peterson, J. R. Observations and modeling of seismic background noise. 1993.

Podolskiy, E. A. Toward the Acoustic Detection of Two-Phase Flow Patterns and Helmholtz Resonators in Englacial Drainage Systems. *Geophysical Research Letters*, 47(6):e2020GL086951, 2020. doi: https://doi.org/10.1029/2020GL086951.

Podolskiy, E. A. and Walter, F. Cryoseismology. *Reviews of Geophysics*, 54(4):708–758, 2016. doi: 10.1002/2016RG000526.

Ringler, A. T., Hagerty, M., Holland, J., Gonzales, A., Gee, L. S., Edwards, J., Wilson, D., and Baker, A. M. The data quality analyzer: A quality control program for seismic data. *Computers & Geosciences*, 76:96–111, 2015. doi: 10.1016/j.cageo.2014.12.006.

Röösli, C., Walter, F., Husen, S., Andrews, L. C., Lüthi, M. P., Catania, G. A., and Kissling, E. Sustained seismic tremors and icequakes detected in the ablation zone of the Greenland ice sheet. *Journal of Glaciology*, 60(221):563–575, 2014. doi: 10.3189/2014JoG13J210.

Röösli, C., Helmstetter, A., Walter, F., and Kissling, E. Meltwater influences on deep stick-slip icequakes near the base of the Greenland Ice Sheet. *Journal of Geophysical Research: Earth Surface*, 121(2):223–240, 2016a. doi: https://doi.org/10.1002/2015JF003601.

Röösli, C., Walter, F., Ampuero, J.-P., and Kissling, E. Seismic moulin tremor. *Journal of Geophysical Research: Solid Earth*, 121(8):5838–5858, 2016b. doi: 10.1002/2015JB012786.

Sergeant, A., Chmiel, M., Lindner, F., Walter, F., Roux, P., Chaput, J., Gimbert, F., and Mordret, A. On the Green's function emergence from interferometry of seismic wave fields generated in high-melt glaciers: implications for passive imaging and monitoring. *The Cryosphere*, 14(3):1139–1171, 2020. doi: 10.5194/tc-14-1139-2020.

Seydoux, L., Shapiro, N., de Rosny, J., Brenguier, F., and Landès, M. Detecting seismic activity with a covariance matrix analysis of data recorded on seismic arrays. *Geophysical Journal International*, 204(3):1430–1442, Mar. 2016. doi: 10.1093/gji/ggv531.

Walter, F., Deichmann, N., and Funk, M. Basal icequakes during changing subglacial water pressures beneath Gornergletscher, Switzerland. *Journal of Glaciology*, 54(186):511–521, 2008. doi: 10.3189/002214308785837110.

Walter, F., Roux, P., Röösli, C., Lecointre, A., Kilb, D., and Roux, P.-F. Using glacier seismicity for phase velocity measurements and Green's function retrieval. *Geophysical Journal International*, 201(3):1722–1737, 2015.

Winter, K., Lombardi, D., Diaz-Moreno, A., and Bainbridge, R. Monitoring Icequakes in East Antarctica with the Raspberry Shake. *Seismological Research Letters*, Apr. 2021. doi: 10.1785/0220200483.